

SUPERCONDUCTING ACCELERATOR RESEARCH AND DEVELOPMENT AT SLAC†

P. B. WILSON, R. B. NEAL, G. A. LOEW, H. A. HOGG, W. B. HERRMANNFELDT,
R. H. HELM AND M. A. ALLEN

Stanford Linear Accelerator Center, Stanford University, Stanford, California, U.S.A.

This paper surveys current and planned research and development at SLAC on superconducting linear accelerators. Ultimately, the goal is to convert the present machine to a two-mile 100-GeV superconducting linac. The technological problems which stand in the way of this achievement are being attacked on two fronts: on the one hand, a better understanding of the properties of superconducting materials, such as residual loss, electric field breakdown and magnetic field quenching is being sought through experiments with individual samples and cavities; on the other hand, many of the design, fabrication and control problems which are the concern of the accelerator builder are being met head-on by the immediate construction of a short superconducting accelerator. The latter project, appropriately named 'Leapfrog', utilizes a 15-cavity niobium traveling-wave resonant ring structure operating in the $2\pi/3$ mode. Many of the parameters for this test accelerator, such as the frequency (2856 MHz) and the accelerating field (33 MV/m), are the same as those envisaged for the two-mile machine. Detailed computer studies have been made to optimize the accelerator structure geometry. The paper concludes with a description of a feasibility study for the proposed two-mile accelerator. Design parameters are discussed and construction schedules and costs are estimated.

1. INTRODUCTION

This report discusses the research and development program now under way at SLAC on superconducting linacs. The principal objective of this program is to establish the feasibility of converting the existing two-mile linear accelerator to a superconducting version of higher energy and improved duty cycle. The possible application of rf superconducting structures to smaller physics-related devices such as beam separators is also of interest.

This paper is intended to be a general survey of the investigations in progress at SLAC involving a large number of individuals. Many technical details cannot be presented here but are or will be available in other published or internal reports.

The large number of basic questions which must be answered before the feasibility of a large high-gradient accelerator can be considered established are discussed in Sec. 2 and some of the experimental work which is now under way or planned for the near future at SLAC is described there.

The shapes of superconducting accelerator structures must be optimized to minimize the ratios of the peak electric and magnetic fields to the effective accelerating fields in the structures. This optimization must be accomplished without significant degradation of the accelerating field itself, and without imposing serious mechanical fabrication problems. The computer-aided procedures

and tentative results obtained at SLAC are discussed in Sec. 3.

The concern that some of the fundamental or practical problems impeding the path to a working accelerator may not be predictable has led to the pursuit of a separate 'brute force' approach in parallel with the fundamental investigations mentioned above. It is hoped, moreover, that this approach may provide answers to some of the questions now considered as potentially serious, and that any unexpected problems which are revealed will turn out to be resolvable. For these reasons, the practical embodiment of this approach, a short test accelerator, is referred to as project Leapfrog. Such a dualistic program with parallel basic and engineering studies has been followed elsewhere, i.e., at the High Energy Physics Laboratory (HEPL) at Stanford. As will be shown in Secs. 3 and 4, the design approach followed in Leapfrog differs significantly from that in other laboratories in that the accelerating structure is a constituent part of a traveling-wave resonant ring rather than being operated as a standing-wave device. However, at this early stage of superconducting accelerator development, SLAC is not irrevocably committed to this design approach.

In addition to these programs, a comprehensive study of the feasibility of converting the two-mile accelerator to a superconducting version with a design energy goal of 100 GeV has been carried out for the past $1\frac{1}{2}$ years.⁽¹⁾ This study has

† Work supported by the U.S. Atomic Energy Commission.

encompassed not only the superconducting structure itself but also the associated systems, utilities, buildings, etc. which would be necessary to achieve a complete accelerator facility. It has also been the goal of this study to examine the economic aspects of various technical approaches to the construction of a 100-GeV accelerator. For this reason, cost factors have been examined in considerably greater detail than might be expected at this stage of technological development.

The selection of the basic parameters for a 100-GeV, two-mile superconducting accelerator is discussed in Sec. 5. A wide variety is possible in the selection of these parameters. One guideline which has been followed is to use as many of the existing machine facilities as possible in order to achieve minimal cost while maintaining scientific utility.

The scientific incentives for undertaking this conversion have been examined⁽¹⁾ but are not given in detail in this article. The much higher energy and duty cycle of the superconducting version of SLAC which is envisioned would open new areas of physics with electron and photon beams. The very important studies of two-body elastic reactions, photoproduction and inelastic electron scattering now in progress in the 20-GeV region could be extended to the higher energies. Intense fluxes of secondary hadron beams would be available to permit SLAC to complement the experimental program at the National Accelerator Laboratory. The availability of a clean neutral K meson beam free of the severe neutron background present at proton accelerators would be an important feature at SLAC. The range of experimental parameters for testing quantum electrodynamics with muon, electron and photon beams would be extended significantly and experimental searches for new electromagnetically-produced particles would become possible.

2. SUPERCONDUCTING MATERIALS STUDIES

General remarks

The program of superconducting materials studies at SLAC is directed toward the goal of developing the relevant technology required to build a two-mile superconducting electron linac. These studies are basic in the sense that a comprehensive understanding of the properties of superconducting materials is necessary if a large superconducting accelerator is to be successfully realized.

Broadly stated, the objectives of the materials studies program are to obtain sufficiently high electric and magnetic breakdown fields in test cavities and small test structures so that an energy gradient of 33 MeV/m can be realized in the two-mile accelerator, and to obtain a sufficiently low surface resistance so that the accelerator can be operated at a high duty cycle (6 per cent or greater) with reasonable refrigeration power. In Sec. 3 it will be shown that, for typical traveling-wave structures operating in the $2\pi/3$ mode at an effective accelerating gradient of 33 MV/m, peak rf electric and magnetic fields of approximately 55 MV/m and 1000 G can be expected at the superconducting surface. Fields of this order have already been attained by Turneure and Viet⁽²⁾ in X-band niobium cavities. An initial goal of the program at SLAC is to obtain similar results in cavities and test structures at both X-band and S-band frequencies. It will also be necessary to obtain a surface resistance at these high field levels which approaches the theoretical value for temperatures in the range 1.5–1.85 °K. For a niobium structure operating in this temperature range, the reduction in loss compared to a room temperature copper structure is expected to be between 10^5 and 10^6 (see comment under Table III), a sufficient reduction to allow a high duty cycle accelerator to be built with reasonable refrigeration requirements. It will not be sufficient to show that these high peak fields and low values of surface resistance can be achieved in a transitory fashion in small test cavities; it must be demonstrated that the required fields and Q 's can be maintained for an operationally significant length of time in slow-wave test structures which have been assembled using practical fabrication techniques.

On the basis of extensive work⁽³⁾ which has already been carried out at the High Energy Physics Laboratory, the required Q 's and field strengths are most likely to be obtained in a structure fabricated from bulk or sheet niobium. The desired superconducting properties are obtained only after the completed niobium cavity or structure has been etched in an acid bath, vacuum fired at a temperature in the range 1600–2000 °C, etched again, and then re-fired at high temperature. There might be some advantage in a superconducting material which can be electroplated or deposited on a copper or aluminum base. Electroplated technetium has been briefly investigated at SLAC, but the results so far are not encouraging. Superconducting alloys such as niobium–tin or niobium–

zirconium, which have been deposited by vacuum evaporation or sputtering, may be investigated later. Such techniques may be useful in the fabrication of auxiliary components where only modest Q 's and field levels are required. The main effort of the program will, however, be concentrated on developing fabrication and processing techniques for solid niobium structures.

In the following paragraphs the superconducting materials research program at SLAC is outlined in more detail. It should be emphasized that research at SLAC in this field is relatively young. This survey is not, therefore, intended to be a summary of experimental results already obtained, but rather is largely a listing of investigations presently in progress or under consideration for the near future. All the measurements are currently being made using X-band TM_{010} and TE_{011} mode cavities. However, as described below, facilities will soon be available for fabricating, processing and measuring cavities and short sections of slow-wave structure at 2856 MHz.

Breakdown fields and residual loss

Many factors affect the residual Q and the limiting fields which can be obtained in a superconducting niobium cavity. To make matters more complicated, a given factor may affect either the Q , the electric breakdown field or the quenching rf magnetic field, or perhaps all three of these parameters at the same time. To completely unweave this tangle of cause and effect relationships will probably prove to be an impossible task, but at least a rudimentary understanding must be strived for. Some of the factors under investigation are: the effect of high temperature processing using various temperature-vs-time cycles on the metallurgical structure and impurity content of the niobium surface, the effect of adsorbed surface contaminants, and the effect of strains in the superconducting material. Because of the importance of the rf magnetic breakdown field in setting an ultimate limit on the energy gradient of a superconducting accelerator, strong emphasis will be placed on a study of this effect. At first sight it might be expected that the rf magnetic breakdown field for a Type II superconductor would be equal to the lower critical field, H_{c1} . Below this field level, flux exclusion is complete and behavior similar to that of a Type I superconductor might be expected.†

† Measurements have shown⁽⁴⁾ that for at least one Type I superconductor (tin), the rf breakdown field is approximately equal to the dc critical field.

Experimental measurements to date, however, have given breakdown fields for niobium which are lower, often considerably lower, than H_{c1} . Recent calculations⁽⁵⁾ indicate that the thermal conductivity in the neighborhood of the superconducting surface may be an important factor in determining the breakdown field. Other factors such as field enhancement by surface roughness or a local reduction of the critical field by impurities or defects may also be important. The physical basis underlying rf magnetic field quenching is not well understood at the present time, and further theoretical and experimental work is required in this area.

Nonlinear effects at high field levels

One of the most important areas currently under investigation is the behavior of the superconducting surface impedance at high field levels. If the surface reactance and surface resistance are dependent on field strength, the resonant frequency of a superconducting cavity can shift and the Q can drop as the excitation level increases. It is important to know the magnitude of these changes in order to design the feedback control systems for stabilizing the phase and amplitude of the fields in the accelerating structure. Preliminary experimental observations on TE_{011} mode cavities indicate that the dependence of the surface reactance on field strength does not exceed the theoretical prediction,⁽⁶⁾ and that for cavities and accelerating structures with practical wall thicknesses, the deflection due to the electromagnetic force acting on the superconducting surface is the dominant effect causing frequency detuning at high field levels.

Radiation damage studies

The susceptibility of the superconducting accelerating structure to radiation damage will be an important consideration in a large superconducting accelerator. Tests are being made in which TE_{011} cavity end plates are irradiated, using both a low energy (≈ 5 MeV) electron beam from a small test accelerator, and the main SLAC accelerator beam. Because the defects produced by radiation tend to anneal out at room temperature, care must be exercised in interpreting these measurements. Tests in which defects are produced directly at liquid helium temperatures, either by electron or ion bombardment, are under consideration.

Other measurements

Several auxiliary measurements are being made at SLAC which complement the rf cavity studies.

Dc field emission studies are useful in interpreting the behavior of niobium surfaces at high rf electric field strengths. An ac susceptibility apparatus has been built which can detect a very small amount of flux penetration into the superconducting surface, and which gives accurate values for H_{c1} . With this apparatus small samples can be measured rapidly and the resultant values of H_{c1} provide a measure of the purity of the material.

It is also important to know the bulk thermal conductivity of the material in a superconducting structure. Poor thermal conductivity will cause a Q degradation at high field levels due to the temperature rise at the inner surface of the structure. Measurements⁽⁷⁾ show that the thermal conductivity of fully processed niobium is about 0.4 W/(cm²·K) at 1.85°K. For a structure with a wall thickness of 0.100 in., at a region where the peak magnetic field is 1000 G, the temperature rise across the wall is about 10 millidegrees for a Q improvement factor of 2.6×10^5 . A temperature rise of this magnitude would cause the surface resistance in the region of maximum magnetic field to increase by about 5 per cent; the resulting degradation in the Q would be even less. The temperature rise due to the Kapitza resistance at the niobium-liquid helium interface must also be considered. Published values for the Kapitza resistance for niobium are lacking. Rough estimates indicate that the temperature rise due to this effect may be several times larger than that due to finite thermal conductivity. Measurements are planned to determine the value of the Kapitza resistance for niobium under conditions approximating its use as a material for an accelerating structure.

Fabrication techniques

It is evident that the superconducting properties of an accelerating structure are critically dependent on the fabrication and processing techniques used in producing the structure. The program of basic measurements on superconducting materials must therefore be closely coupled with an investigation of possible fabrication techniques.

The technique currently favored for building long lengths of slow-wave structure is to make half-cells from niobium sheet stock by forming the sheet against a die using one of several processes, and then to electron beam weld the half-cells together at the major and minor diameters of the structure. The general technique was first developed at HEPL, and, in particular, measurements there have shown⁽²⁾ that high Q 's and high fields can be obtained in an

electron beam welded cavity. We expect to exploit the electron beam welding technique at SLAC, and X-band cavity tests are in progress to determine the losses and critical fields for these welds under a variety of conditions. In particular, it is of great interest to measure the critical fields that can be obtained in niobium subassemblies which are welded together after having been fully processed. This technique will be useful in cases where further high temperature processing is not feasible because of the size of the resulting assembly. It is hoped that welding under high vacuum conditions (on the order of 10^{-7} torr) will produce welds with lower losses and higher critical fields.

Other joining techniques such as diffusion bonding, rf induction brazing with vanadium, and TIG welding are also under investigation. Techniques which are not adequate for the high field accelerating structure itself may still be useful for joining parts in lower field regions, such as the feedback waveguide.

Various methods for fabricating the niobium half-cells from sheet material are being studied. Among the many possibilities are hydroforming, Electroshaping,[†] coining, stamping, spinning, die forging, or perhaps several of these operations in some combination. At present the Electroshaping process, in which sheet stock is literally smashed against a die by a shock wave generated by a high energy electric spark in a liquid, looks particularly attractive. The material acquires the shape and finish of the die with practically no spring-back. Cavity tests are being performed to determine the effects of the high strain rates involved in this process.

Fabrication and processing facilities

Because electron beam welding and high temperature processing are vital techniques in the production of successful niobium cavities and structures, it is highly desirable to have an in-house capability to carry out these operations. A Hamilton-Standard 25 kW electron beam welder is now operational at SLAC, and a new rectangular vacuum chamber 5 ft wide by 5 ft high by 9 ft long, which will operate at a base pressure of 10^{-7} torr, is under construction for use with this welder. With this chamber, welds can be made on cavities or long test structures under improved vacuum conditions.

At the present time, X-band cavities and small niobium pieces are processed by induction heating

[†] Trademark of Cincinnati Shaper Company.

inside a quartz vacuum envelope. Because of the growing need for processing larger cavities and assemblies, a high temperature (up to 2000 °C), high vacuum (10^{-9} torr) furnace with a hot zone approximately 7 in. in diameter by 12 in. in length is being built. With this furnace S-band cavities and subassemblies for project Leapfrog (see Sec. 4) can be processed.

3. ACCELERATING STRUCTURE STUDIES

The accelerating structure being developed for a superconducting accelerator at SLAC is a $2\pi/3$ mode traveling-wave (TW) resonant ring. There are several reasons for developing such a structure although it is by no means certain that a resonant ring will be chosen when the proposed conversion program is carried out. The most important reason is that the TW resonant ring holds the promise of the highest possible energy gradient. Also, since other laboratories that are experimenting with superconducting accelerators are working on standing-wave (SW) structures, it appears worthwhile to develop the TW system to gain the experience and to have a basis of comparison. The fact that the chosen frequency (2856 MHz) and mode ($2\pi/3$ TW) are both the same as those presently used at SLAC may be partially the result of a predilection for these values in this laboratory. However, an elaborate series of calculations have indicated that the $2\pi/3$ TW structure is close to if not the optimum structure for the most favorable ratio of peak electric and magnetic rf fields to the effective accelerating field.

Computer-aided design studies

Two computer programs with entirely different approaches were used to calculate the parameters of the accelerator structure. The first program is a new Fortran version of the LALA^(8,9) program written at the Los Alamos Scientific Laboratory. This program is a mesh calculation leading to a numeric solution of the fundamental mode of a cylindrically symmetric resonant cavity. The program was written for CDC Fortran and adapted here for use on the SLAC IBM 360 Model 91 computer. Since this program is intended for standing-wave solutions, certain corrections have to be made to the data to make it appropriate for a TW structure.

A second program called TWAP⁽¹⁰⁾ (Traveling-Wave Accelerator Program) was written expressly

for the purpose of computing TW structure parameters. TWAP uses an expansion in TW modes with appropriate matching of boundary conditions to calculate the fields and other parameters of a TW structure. Besides yielding TW results directly, TWAP has the advantage that it can calculate modes with an arbitrary phase shift per cavity and also calculate the group velocity.

The shape of the accelerator structure was arrived at by optimizing various parameters within limits given by a number of practical restrictions. The minimum aperture is limited by considerations of coupling and of beam dynamics.

The cylindrical symmetry required by both computer programs rules out making calculations for any nonsymmetric structure such as the side-coupled cavity used by Los Alamos for LAMPF or other exotic structures such as the 'jungle gym'. It is probable that the local peak magnetic fields would be appreciably higher in such structures and thus they would be undesirable for a superconducting accelerator.

Other restrictions relate to problems of cooling and fabrication. Even a 0.1 °K rise in the internal surface temperature can cause about a 50 per cent reduction in the cavity Q . Thus it is important to keep the wall fairly thin and to avoid solid disks where the heat path is too long for adequate cooling.

The way in which the LALA code can be used for TW calculations, particularly in the $2\pi/3$ mode case, is illustrated by Fig. 1. By choosing the

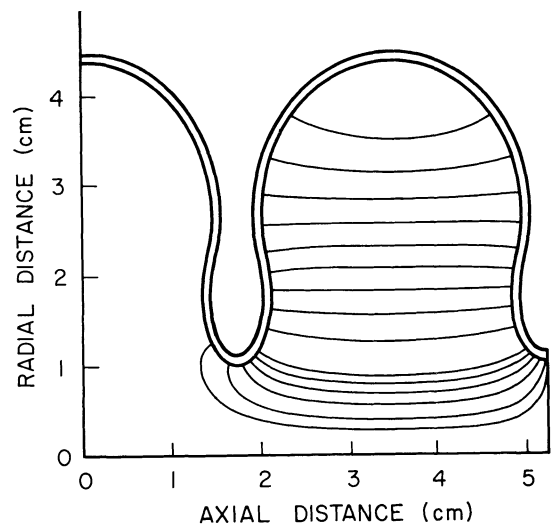


FIG. 1. 'Bulgy disk' cavity planned for the Leapfrog test accelerator. Field lines shown are calculated by LALA.

'cavity' for the program as $1\frac{1}{2}$ accelerator cavities, it is possible to run the program in a π mode. The field lines shown in the figure are in the direction of the electric field but the density of the field lines does not indicate the relative strength of the electric field. This is because these lines are actually lines of constant rH_ϕ . Since LALA is a SW program, the calculated results show the left hand half-cavity to be always relatively unexcited and the highest electric field to be on the disk tip on the right. For $2\pi/3$ TW, all cavities are, of course, equally excited by a wave which has a $2\pi/3$ phase shift from one cavity to the next. The corresponding points in two successive cavities can be considered to have fields of equal amplitude but $2\pi/3$ radians out of phase. The SW calculation can be used to calculate the TW fields by considering any two corresponding points in the two cavities. Then the field A_{TW} is given by

$$A_{TW} = \frac{(A_1^2 + A_2^2 - 2A_1A_2 \cos^2 kl)^{1/2}}{2 \sin kl}$$

where A_1 and A_2 are the SW fields at the two points and kl is the phase shift between the two points. For the $2\pi/3$ case,

$$A_{2\pi/3} = (A_1^2 + A_2^2 - A_1A_2/2)^{1/2}/\sqrt{3}$$

When the two points are chosen so that one is in a region of very low field, as is the case here, then for all practical purposes the equation reduces to

$$A_{2\pi/3} = A_1/\sqrt{3}$$

where A_1 is in the high field region. Figure 2 shows the axial (SW) electric field for the cavity of Fig 1. From Fig. 2 it is apparent how low the fields are in the unexcited cavity.

Results obtained for specific structures

Three basic structures were used in the series of calculations. First was the traditional 'SLAC Type' structure with a flat disk and a cylindrical wall. Substantial improvements were made in Q and in the ratio of peak electric field to effective accelerating field (\hat{E}/E_{eff}) by rounding the wall of the cylinder at the point where it joins the disk. This led to the second basic structure called 'Tapered Disk' in which the disk tip and the top of the cylinder are elliptical. This structure is shown in Fig. 3. Further improvements in both Q and r/Q (where r is the effective shunt impedance) were made by increasing the thickness of the disk tip and by reducing the minimum disk thickness, as shown in Fig. 1, and described as 'bulgy disk'. If the disk

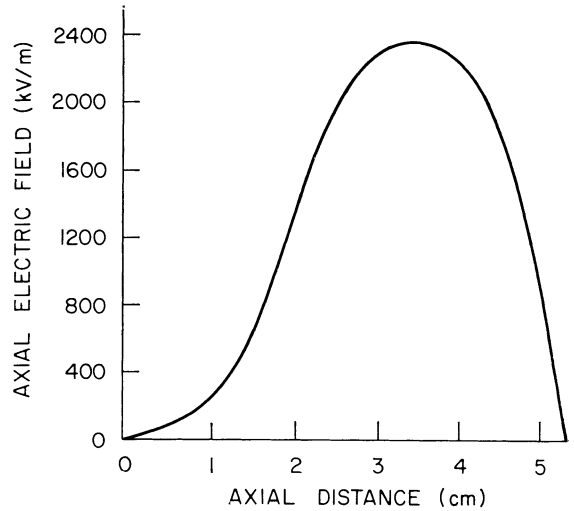


FIG. 2. Axial standing-wave electric field for the cavity shown in Fig. 1.

could have been made even thinner, greater improvement would have resulted. However, the thickness required by the two walls and the possible need to get an electron beam between the walls to make the weld at the disk tip determines the minimum disk thickness. Any significant increase in the bulge thickness increases the peak magnetic field and thus is not desirable. The results of the above procedures are summarized in Table I.

The best argument for the choice of the $2\pi/3$ TW structure comes from TWAP results for different

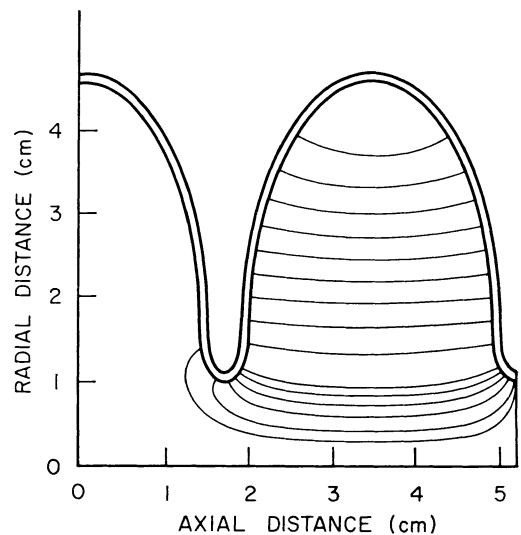


FIG. 3. Tapered disk structure with field lines as calculated by LALA.

TABLE I
Computer results for $2\pi/3$ copper structures

	Bulgy disk		Tapered disk	
	LALA	TWAP	LALA	TWAP
f (MHz)	2856.6	2856.1	2856.2	2856.0
Q	15,149	15,040	14,493	14,460
r (M Ω ,m)	65.9	65.4	60.8	59.7
\hat{E}/E_{eff}	1.65	1.61	1.75	1.66
\hat{H}/E_{eff} [G (MeV/m)]	30.5	30.2	30.9	31.1
r/Q (Ω ,cm)	43.4	43.5	42	41.3
v_g/c		0.0071		0.0078

phase shifts per cavity. These results are shown in Table II for the 'Tapered Disk' copper cavity.

The general conclusion to be drawn from Table II is that the optimum structure is somewhere between $\pi/2$ and $3\pi/4$. The $2\pi/3$ structure is somewhat cheaper than the $\pi/2$ structure and so, for this and for the reasons given earlier, it is the choice at this time.

Deformation due to rf fields

With the interest in high-field, high- Q structures, particularly with thin walls, it becomes important as discussed in Sec. 2, to consider the frequency shift due to wall deformations caused by the rf fields themselves. Such frequency shifts will produce small changes in the phase shift per cavity and cause the ring to drop slightly out of resonance. The tuning system, which must correct for this shift, has a fairly narrow range and thus restricts the amount of detuning permitted.

The detuning of the cavities has been calculated by Cochran using a computer program⁽¹¹⁾ designed to evaluate small deflections in bellows. Figure 4 shows the deflection of a 'bulgy disk' cavity with 0.075 in.-thick walls. The calculation includes a

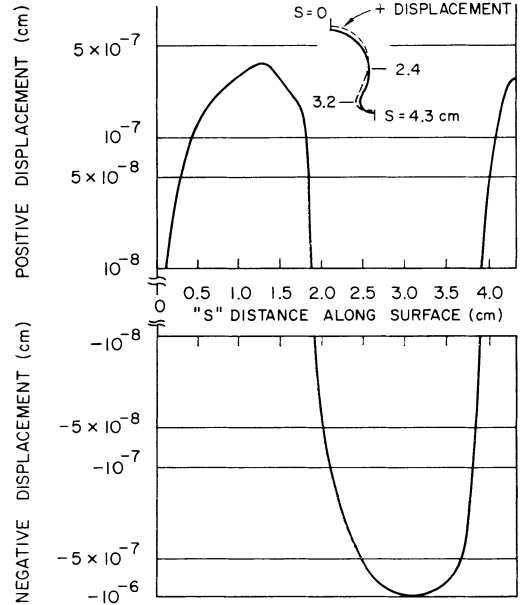


FIG. 4. Wall deflections of the 'bulgy disk' structure with a wall thickness of 0.075 in. and a guard tube of 0.050 in. thick niobium.

guard tube of 0.050 in. thickness which is attached at the outer diameter. The calculated frequency shift of this configuration appears to be about 430 Hz. The pressures on the walls are found from the fields calculated by LALA. The rms pressure is

$$P_{\text{rms}} = \frac{1}{4} \left(\frac{B^2}{\mu_0} - \epsilon_0 E^2 \right)$$

where B and E are the peak fields in the TW mode, i.e., the calculated SW field divided by $\sqrt{3}$. The work done, δU , is found by integrating the pressure over the small volume of distortion, $d\tau$,

$$\delta U = \frac{1}{4} \int_{\tau} \left(\frac{B^2}{\mu_0} - \epsilon_0 E^2 \right) d\tau$$

TABLE II
TWAP results vs phase shift per cell for copper structures

kl	$\pi/2$	$2\pi/3$	$3\pi/4$	$5\pi/6$	π
$l/2$ (cm)	1.3125	1.7500	1.9687	2.1875	2.6250
b (cm)	4.7213	4.6851	4.6696	4.6549	4.6259
r/Q (Ω ,cm)	44.2	41.3	38.6	35.5	28.6
Q	10,770	14,460	16,090	17,590	20,250
r (M Ω ,m)	47.6	59.7	62.2	62.5	57.9
v_g/c	0.00925	0.00784	0.00630	0.00437	0
\hat{E}/E_{eff}	1.561	1.661	1.768	1.884	2.096
\hat{H}/E_{eff} [G (MeV/m)]	31.5	31.1	31.5	32.3	35.2

The frequency shift is found from the expression

$$\delta\omega/\omega = -\delta U/U$$

where U is the total TW stored energy in the cavity ($\frac{1}{2}$ of the SW stored energy).

These results are very preliminary and a great deal of further work is required. There is at this time no experimental verification of these calculations. However, the problem is sufficiently serious to warrant continued study and to require careful attention to the way in which the cavity is braced to reduce the deflection as much as possible.

4. PROJECT LEAPFROG

As discussed in the introduction, the object of project Leapfrog is to leap over some of the fundamental investigations presently under way and to achieve the construction of a 50-cm test accelerator in a relatively short time span. Construction of this accelerator is planned in two stages: (1) without a beam, and (2) with a beam. It is expected presently that the schedule for stage (1) will occupy most of calendar year 1970. Stage (2) is already in the planning phase but actual construction will not proceed until stage (1) is fairly well advanced.

Design parameters of the traveling-wave resonant ring

As discussed in Secs. 1 and 3, the traveling-wave resonant ring appears to have several advantages over standing-wave structures for superconducting accelerators. Leapfrog is to provide the first feasibility test of a superconducting resonant ring.

The theory of traveling-wave resonant ring accelerators has been discussed elsewhere^(12,1) and will not be reproduced here. However, it seems worthwhile to describe briefly how the principal Leapfrog parameters have been arrived at (see Table III). The length of 15 cavities or 52.5 cm has been chosen arbitrarily. Since Leapfrog is to serve as an early test vehicle for the two-mile conversion program, many of the key parameters given in Sec. 5 will be used here. These include the frequency (2856 MHz), the energy gradient (32.8 MeV/m or 17.2 MeV for 52.5 cm) and the klystron power P_s (1.64 kW/m or 860 W for 52.5 cm). The values of the Q improvement factor and r are based on 'reasonable' expectations derived from measurements⁽²⁾ at the Hansen Laboratories. The design current is 48 μ A. The bridge ratio (g) or coupling coefficient C of the feed coupler, where $C = 1/g$, has been determined as follows.

From Ref. 1 and referring to Fig. 5, the steady-

TABLE III
Leapfrog design parameters

Length	52.5 cm
Frequency	2856 MHz
Energy gradient (max)	32.8 MeV/m
Design loaded energy	17.2 MeV
Klystron power (cw)	≥ 860 W
r/Q	43.5 Ω /cm
v_g/c	0.007
Q estimated ^a for Nb at 1.85 °K	4×10^9
Q improvement factor	2.6×10^5
r	1.72×10^{13} Ω /m
$\tau = \alpha l$	5.7×10^{-7} nepers
Design beam current	48 μ A
Loop feed coupling	~ 45 dB
Bridge ratio g	$\sim 36,000$
$2\tau g$	4.1×10^{-2}
$\beta = 1/(2\tau g)$	24
Q_L	1.5×10^8
$t_f = 2Q_L/\omega$	16.8 msec
Circulating power with beam ($i = 48 \mu$ A)	30 MW
Load power with beam ($i = 48 \mu$ A)	0
Load power without beam	~ 800 W

^a The values of Q and the improvement factor quoted here were calculated as follows. At 2856 MHz and low field, J. Turneure (private communication) has calculated an improvement factor of 4.7×10^5 at 1.85 °K. This would yield a Q of 7.1×10^9 for the 'bulgy disk' niobium structure. However, it is expected that nonlinear effects at high field levels will reduce the Q below this value. Adequate theoretical calculations of these effects have not yet been published. Experimental measurements² at high fields and 1.25 °K indicate that the reduction factor will be slightly greater than 2 at 1000 G. At 1.85 °K the reduction factor is expected to be somewhat lower (J. Turneure, unpublished calculation) and we have therefore taken 1.8 as a reasonable expected value. This reduction factor leads to a Q of 4×10^9 and an improvement factor of 2.6×10^5 .

state energy of the beam for the resonant ring is given by

$$V = \left\{ \frac{[4/(2\tau g)]rIP_s}{[1 + 1/(2\tau g)]^2} \right\}^{1/2} - \frac{rli}{1 + 1/(2\tau g)}$$

where g , P_s , r and l have been defined above and τ is the attenuation length:

$$\tau = \frac{\omega l}{2v_g Q} = \frac{\pi(l/\lambda)}{(v_g/c)Q}$$

The energy can also be expressed⁽¹⁾ in terms of the coupling coefficient β :

$$V_{TW} = \left[\frac{4\beta}{(1 + \beta)^2} rIP_s \right]^{1/2} - \frac{rli}{1 + \beta}$$

By analogy between the two formulas, it is seen that $\beta = 1/(2\tau g)$.

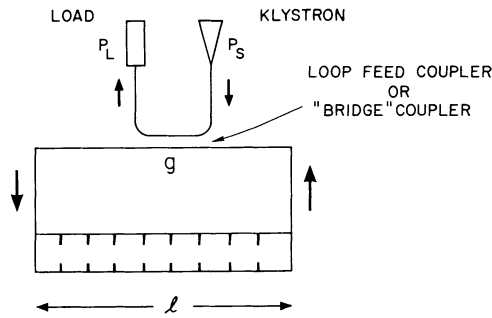


FIG. 5. Schematic of a traveling wave resonant ring.

For maximum efficiency, the design energy is one-half the no-load energy. Using the above equations and assuming large β , it can be shown that under this condition

$$\beta = \frac{1}{2\tau g} = \frac{r(P_s/l)}{(V/l)^2} - 2$$

and

$$\frac{1}{g} = C = \frac{2\pi(l/\lambda)(P_s/l)(r/Q)}{(v_g/c)(V/l)^2}$$

Inserting numerical values into these equations, it is found that $g \approx 36,000$, $C \approx 45$ dB, $\tau = 5.7 \times 10^{-7}$, $2\tau g \approx 4.1 \times 10^{-2}$ and $\beta \approx 24$. As expected, the ring is highly overcoupled in the absence of the beam.

For large β , the loaded Q of the system is given by

$$Q_L \approx \frac{(V/l)^2}{(P_s/l)(r/Q)} \approx Q_0(2\tau g) \approx \frac{Q_0}{\beta}$$

and the filling time, t_f , required to fill the ring to 63.2 per cent of full field level is given by

$$t_f = \frac{2Q_L}{\omega} \approx \frac{2Q_0}{\omega} (2\tau g) \approx \frac{2Q_0}{\omega\beta}$$

It is seen that Q_L is fixed once the energy gradient, the klystron power per unit length and r/Q are chosen. The numerical values of Q_L and t_f appear in Table III.

The duty cycle for Leapfrog could be as high as 100 per cent and the 'time on' will be limited only by the helium capacity of the dewar and the pumping speed. After resonant operation of the ring has been achieved successfully, it will be possible to test various schemes that have been proposed for rf level control. In stage (1), in the absence of any beam, the circulating power in the ring would rise to four times the 30 MW level (to 120 MW) and the field level for either magnetic or electric breakdown would be exceeded. To prevent this

from occurring, one could either reduce the klystron output level or pulse the rf drive input to the klystron.

Design of Leapfrog components

For ease of construction, stage (1) of Leapfrog will be installed in a vertical dewar. A layout of the proposed assembly is shown in Fig. 6. The dewar will be approximately 2 ft in diameter and 5 ft high. The design is fairly conventional.

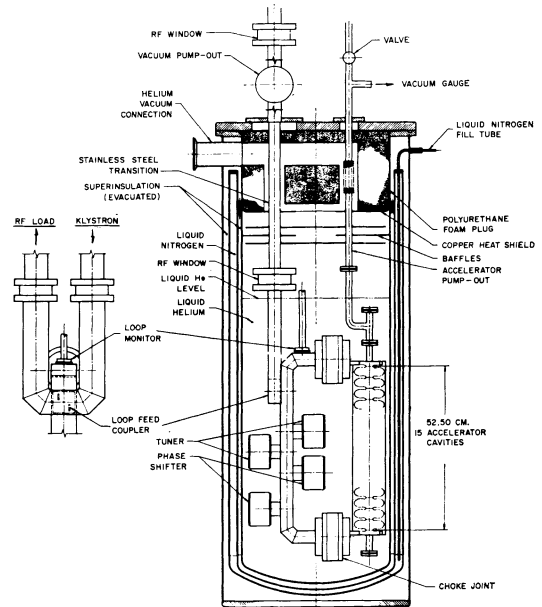


FIG. 6. Dewar assembly for the Leapfrog test accelerator.

The resonant ring consists of several parts. Seen to the right is a 15-cavity niobium, slow-wave structure (52.5 cm long). As described in Sec. 3, each cavity is 3.5 cm long ($2\pi/3$ mode) and has curved boundaries with 'bulgy disks' to minimize peak-to-effective field ratios. The wall thickness of the cavities will be of the order of 0.075 to 0.100 inches. The structure is surrounded by a niobium guard tube which serves as a stiffener.

Coupling into and out of the slow-wave structure is achieved by means of two coupler cavities at the ends of the structure. The design of these couplers is a marked departure from the conventional magnetic coupling iris design used at SLAC and resembles more closely the design used at Orsay.⁽¹³⁾ The reason for this change is that calculations have shown that the presence of the coupling iris increases the peak-to-effective magnetic field ratio by about 50 per cent and thus sets an undesirable upper limit

to the operating level of the entire structure. In the proposed design, the coupler cavity is simply an extension of the conventional rectangular waveguide (2.84 in. by 1.34 in.) reduced to one-quarter height. For matching and field symmetry purposes, three parameters can be adjusted: the location of the point where the waveguide steps down to 1/4th height, the location of the back-end short and the diameter of the first iris. The upper cutoff hole, eventually to be used for the beam, presently serves as pumpout and port for a vacuum gage. The lower hole is to be capped off.

The return loop, as already mentioned, consists of rectangular waveguide fabricated from $\frac{1}{8}$ in. niobium sheet. The waveguide is joined to the structure by means of two choke joints. As shown, it includes a feed coupler, a monitor coupler and four plungers. The total electrical length of the loop will probably be 12 wavelengths. The choke joints are actually double joints between which niobium spacers can be inserted to obtain an integral number of wavelengths around the loop. The feed coupler, as discussed earlier, is a 45 dB cross-guide coupler with 40 dB or better directivity. Similarly, the monitor coupler is a 70 dB waveguide-to-coax coupler with a directivity of at least 40 dB. With 30 MW circulating in the loop, the output of this coupler will be 3 W which should be adequate for all control features.

Two pairs of plungers are provided. The lower pair provides both coarse and fine phase adjustments around the loop. The upper pair provides coarse and fine tuning to match out any residual reflections. At the present time, it is believed that all four plungers will be of identical construction (see Fig. 7). Briefly, each plunger consists of a 1.0 in. diameter piston attached to the broad wall of the rectangular waveguide. The effect of this plunger is to produce 12 millidegrees of phase shift per 0.001 in. of travel. The plunger is driven in and out by a piezoelectric disk (lead zirconate-titanate) which bends when a voltage is applied across it. Deflections of the order of 0.001 in./800 V have been obtained at liquid helium temperatures. The desired specifications per plunger are:

- Resolution: Phase $\sim 8 \times 10^{-6}$ degree
 Reflection coefficient $\sim 5 \times 10^{-8}$
 Fine Range: Phase $\sim 1.6 \times 10^{-2}$ degree
 Reflection coefficient $\sim 1 \times 10^{-4}$

In order to make coarse adjustments, it will also be possible to move the plungers slowly through a range of ± 0.125 in. This displacement corres-

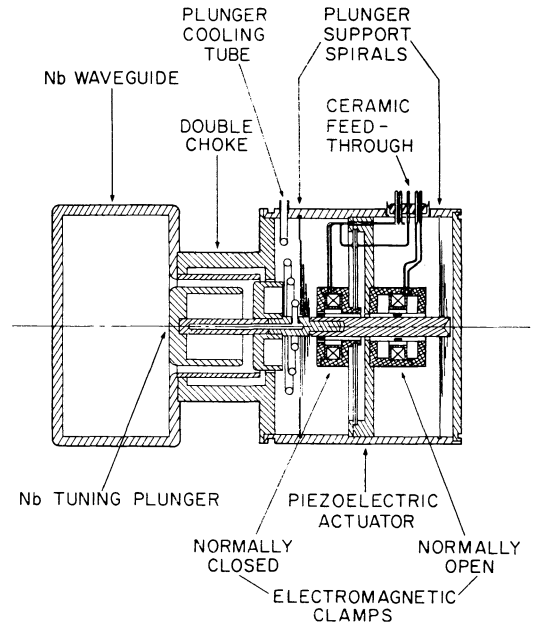


FIG. 7. Plunger and plunger actuator for the Leapfrog test accelerator.

ponds approximately to a phase excursion of $\pm 3^\circ$ for a pair of plungers or a reflection coefficient change of 0.026 (VSWR ~ 1.05). The displacement is to be achieved by combining the piezoelectric disk with two electromagnetic clamps which alternately clamp and release the plunger shaft, forming a linear stepper motor or 'incher'. A prototype of the incher mechanism has been built and operated at room temperature. Also, a double choke has been designed to prevent excessive rf power leakage into the plunger housing.

As mentioned above, the plungers are provided in two pairs. In the lower pair, they are spaced $(3/4)\lambda_g$ apart so that the combination may produce a phase shift without reflection. In the upper pair, they are spaced $(3/8)\lambda_g$ apart so that the reflections produced are orthogonal.

The ring vacuum will be isolated by means of two sets of ceramic windows. Thin-wall stainless steel waveguide sections will be used for thermal isolation. As seen in Fig. 6, the klystron output will be connected to one arm of the coupler and the rf load to the other. Since the rf load is external to the dewar, any power not coupled into the ring will be dissipated at room temperature.

The rf driver chain will consist of an ultra-stable (one part in 10^{10}) S-band oscillator followed by a pin-diode modulator. This modulator will allow control of the on-time and the off-time of the drive

power into the klystron at a rate fast compared to the filling time in order to obtain a desired level of excitation of the ring. It should be noticed that in stage (1), the rf losses in Leapfrog are only wall losses and consequently the klystron drive will be turned on only about 50 per cent of the time.

The electronics system with the feedback controls, which will 'phase', 'match' and 'level adjust' the rf in the ring, is beyond the scope of this report and will not be discussed here. A summary of the functions is given in Sec. 5.

As mentioned earlier, the schedule for stage (1) of Leapfrog is expected to extend to the end of 1970. However, plans have already been started for stage (2). The resonant ring presently under design and construction as described above will be used again if it operates satisfactorily. In any event, a new horizontal dewar with input and output beam holes will have to be built. The injection system will use a modified SLAC electron gun capable of 1 mA continuous current. It will be followed by a cw room temperature prebuncher and possibly a beam chopper. At the output of the section, there will be a momentum analyzing magnet capable of handling beam energies up to 20 MeV. Beam dumps and shielding are presently under study. In addition to measuring the usual beam parameters, such as energy, beam loading effects, etc., it is planned to study the beam breakup instabilities which may arise spontaneously. For purposes of study, the breakup may have to be stimulated by means of an externally excited in-line resonant cavity. It is expected that this part of the program will extend into at least the first six to nine months of 1971.

5. FEASIBILITY STUDY FOR A TWO-MILE SUPERCONDUCTING ACCELERATOR

As stated in Sec. 1, considerable effort has been devoted to a study of the feasibility of converting the existing two-mile accelerator to a superconducting machine.^(1,14,15) Since the scientific, technical and economic factors are individually dynamic and mutually interacting, this study must necessarily be a continuing one. Although the final values of the basic machine parameters may change considerably as the study progresses, a tentative set of parameters is given in Table IV.

Choice of frequency

Preliminary design studies and cost analyses have been carried out at two frequencies, 1428 and

TABLE IV

Parameters of a two-mile 100 GeV superconducting accelerator^a

Operating frequency	2856 MHz
Length	3000 m
r	$1.72 \times 10^{13} \Omega/m$
Q	4.0×10^9
Loaded energy (max)	100 GeV
Duty cycle	1/16
Peak beam current	48 μ A
Average beam current	3 μ A
Peak beam power	4.8 MW
Average beam power	0.3 MW
Number of klystrons	240
Peak power per klystron	20 kW
Average power per klystron	1.25 kW
Type of rf structure	TW with rf feedback loop
Number of accelerator sections	480
Length of accelerator section	20 ft
Filling time (to 63.2%)	18 msec
Power dissipated in accelerator	12,000 W (4.0 W/m)
Pulse length (rf)	0.25 sec
Pulse length (beam)	0.24 sec
Time off between rf pulses	3.75 sec
Accelerator attenuation factor (τ)	37.0×10^{-7} nepers
Feedback attenuation factor (γ)	3.7×10^{-7} nepers
Bridge ratio (g)	0.546×10^4
Circulating power P_0 at η_{max}	54.6 MW

^a The values of parameters in this table are based upon operation at 100 GeV. The ranges of these parameters for other beam energies are shown in Fig. 8 assuming constant rf dissipation in the accelerator.

2856 MHz. The lower frequency has the advantage of higher Q , lower rf losses, and thus lower refrigeration costs. It also results in larger beam aperture. On the other hand, the higher frequency, 2856 MHz, results in a physically smaller structure and has the advantage that it is the same as the frequency of the existing accelerator. Thus, substantial cost savings could result from the utilization of parts of the waveguide system which are already in place. The complete cost study predicts net savings of more than 10 per cent at the 2856 MHz frequency. For this reason, a tentative decision has been made to adopt this higher frequency, and the parameters given in Table IV are based upon operation at 2856 MHz.

Electron beam energy

An energy goal of 100 GeV has been chosen since this energy is sufficiently higher than the 20-GeV capability of the present SLAC accelerator to be of great interest in physics research and yet within anticipated fiscal and technical limitations.

Test results to date indicate that the voltage gradient (33 MeV/m) required to achieve the 100-GeV design goal will be difficult to achieve. For this reason, the tentative decision has been made to utilize a traveling-wave resonant ring structure (see Secs. 3 and 4). As has been mentioned earlier, this decision is not irreversible. At the present time, it is possible to design π -mode SW structures for which the peak-to-effective field ratio is only about 15 per cent worse than for the TW structure proposed here. However, since the field flatness in a π -mode structure is sensitive to perturbations caused by machining errors and by adjustable tuners, a structure of any appreciable length would require unexcited resonant coupling cells at periodic intervals. Because of the presence of such unexcited cells, and because the field level in cells having coupling apertures or tuning devices may have to be lowered due to magnetic field enhancement in these regions, the peak-to-effective field ratio will be significantly higher than for a single ideal π -mode cell. Values of this ratio which are 20 to 30 per cent higher than for TW structures seem realistic.

Duty cycle

High duty cycle is a principal feature of the superconducting accelerator. The required capacity of the refrigeration system is, of course, directly related to the duty cycle. For economy, it is planned to limit the duty cycle initially to 1/16 (~ 6 per cent) when the machine is operating at the full design level of 100 GeV. This duty cycle is 100 times greater than that of the existing two-mile accelerator. At a later date, the duty cycle could be further increased if technological advances result in a decrease in refrigeration costs or if operation at a lower temperature results in an increase in Q and a corresponding decrease in refrigeration demand.

The rf dissipation varies as V^2 , where V is the electron beam energy. Thus, as the energy is decreased, the duty cycle can be proportionally increased for a given total refrigeration capacity. For example, at an energy level of 25 GeV, the duty cycle can be as high as 100 per cent without exceeding refrigeration limits. Curves of maximum duty cycle, peak and average beam current, and peak and average beam power are shown vs beam energy in Fig. 8. From these curves, it may be noted that, while the average beam power is limited to 300 kW at the design energy level of 100 GeV, the beam power can be higher at lower energies. The maximum beam power (2.1 MW) is obtained at 25 GeV, 84 μ A and unity duty cycle. The dotted lines in

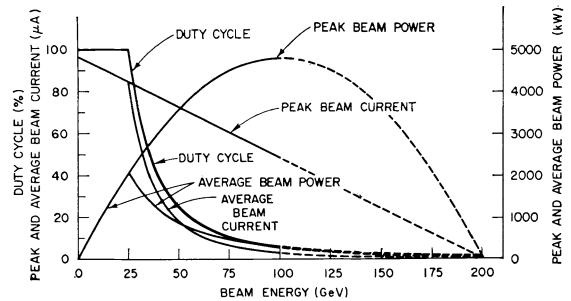


FIG. 8. Duty cycle, peak and average beam power, and beam current vs energy.

Fig. 8 show maximum beam performance at beam energies higher than the 100 GeV design level. The no-load energy is 200 GeV. However, present theory and measurements indicate that field emission or the critical magnetic field will limit the energy to a lower level.

To achieve the proposed beam parameters of the superconducting accelerator, a total peak rf power of 4800 kW is required. The same number of klystrons (240) used in the present two-mile accelerator will be employed in order to take maximum advantage of existing waveguide and power facilities. Each tube must therefore supply a peak power of 20 kW.

Capabilities of ac and rf systems

As noted in Table IV, the filling time of the superconducting accelerator is 18 msec, which is very long compared to the filling time of conventional accelerators. The proposed rf pulse length (0.25 sec) is many times longer to allow time for buildup of fields and acceleration of particles. When an rf power source (such as a klystron amplifier) is designed to produce pulses of this length, it can in practice operate continuously (cw) without exceeding heat dissipation or cathode emission limitations. Moreover, the ac distribution system already existing in the Klystron Gallery has sufficient capacity to supply 240 klystrons of the proposed design (assuming ~ 50 per cent efficiency) when they are operating in a cw manner. Thus, the rf facility will have cw capability from the outset although, as noted above, the initially installed refrigeration system capacity will limit the duty cycle at 100 GeV to ~ 6 per cent.

Field stabilization

Means must be provided to maintain the field strength level in the accelerator loops at the desired

value. This level can vary because of many factors including: (1) variations in klystron output, (2) klystron and loop phasing errors, (3) loop mismatch errors, and (4) beam current variations. It is possible, in principle, to maintain the field strength constant (except for transient effects) by adjustment of the beam voltage or the rf drive of the klystrons. However, these methods cause unwanted phase shifts in the klystron output. Another method, which has been tentatively adopted, consists of comparing the field level in the feedback loop with an adjustable sawtooth reference level having a periodicity of 20 μsec . The rf power is automatically turned on when the level in the loop is less than the level of the sawtooth reference voltage and turned off when it exceeds the reference voltage. Calculated values of the 'on' and 'off' periods for a beam energy of 100 GeV and a klystron peak power output of 20 kW per tube are given in Table V. These values would, of course, be different for other values of beam energy and klystron power. However, in all cases the sum of the 'on' and 'off' periods will be 20 μsec . Using this method, it should be possible to maintain the field level in the loop constant within ± 0.05 per cent or better (at an energy of 100 GeV) over the entire range of beam current between 0 and 48 μA .

Description of rf system

As shown in Table IV, a 20-ft feed interval has been adopted. Thus, each klystron feeds two 20-ft accelerator sections. This arrangement permits the future possibility of doubling the maximum beam power by connecting twice as many klystrons as initially provided to the accelerator through waveguides already in existence.

TABLE V
Rf on-off periods for field stabilization^a

Beam current	[Beam current / Design current]	Length of 'on' and 'off' periods during steady state portion of rf pulse	
		ON	OFF
0	0	10 μsec	10 μsec
12 μA	0.25	12.5 μsec	7.5 μsec
24 μA	0.50	15 μsec	5 μsec
36 μA	0.75	17.5 μsec	2.5 μsec
48 μA	1.00	20 μsec	≈ 0 μsec

^a For beam energy of 100 GeV and klystron power of 20 kW.

The rf system of the superconducting accelerator will consist of 240 20-kW klystron amplifiers supplied from a two-mile 476 MHz coaxial drive line and a common master oscillator having a stability of 4×10^{-10} . Intermediate parallel stages of amplification and multiplication ($\times 6$) will be provided.

Features of accelerator sections and sectors

The conceptual design of a 20-ft section of the traveling-wave accelerator with feedback is shown in Fig. 9. At steady-state design conditions (100-GeV energy, 48 μA beam current, and 10 kW input to each 20-ft section) all the rf power is fed into the accelerator structure and no power goes to the rf load. During the transient filling time and when operating at other than design conditions, some power goes to the load. For this reason, the load is situated outside of the liquid helium dewar in which the accelerator structure is located. Devices

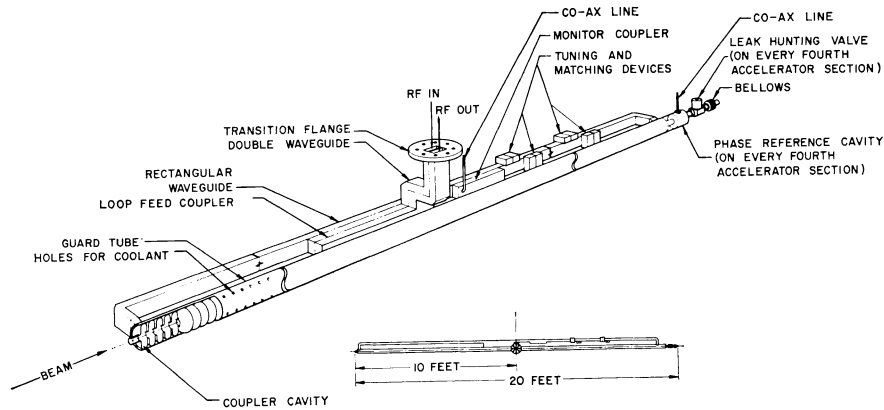


FIG. 9. Conceptual layout of 20-ft section with rf feedback loop.

are provided in the feedback waveguide to help accomplish the following functions on a continuous basis: (1) the rf length of the loop is adjusted to be an integral number of wavelengths by means of phasing transducers; (2) the rf reflections in the loop are minimized by means of matching transducers; (3) the phase of the klystron is optimized with respect to the phase of the beam by comparing the phase of a signal from the input waveguide to the accelerator with the phase of a signal from a phase reference cavity in line with the beam; and (4) the rf field level in the loop is maintained at the desired level by comparing the amplitude of a signal derived from the forward wave in the loop with the amplitude of an adjustable reference level and controlling the rf 'on' and 'off' times as discussed previously. All of these functions will be accomplished by means of automatic closed-loop control circuits.

The superconducting accelerator will be divided into 30 sectors as in the case of the present two-mile accelerator. Each sector will consist of sixteen 20-ft accelerator sections housed inside a 320-ft stainless steel dewar which is 30 inches in overall diameter. Concentrically located inside of the outer vacuum tank are a helium tank 18 in. in diameter and a heat shield 24 in. in diameter. High performance insulation and the heat shield are used to insulate the helium tank which is maintained at a temperature of 1.85°K. Helium gas from the refrigeration system at a temperature of 80°K will be used to cool the heat shield. The refrigeration required to cool the shield amounts to only 2 to 4 per cent of the total refrigeration load. The feed-throughs and supports are designed for minimum heat leakage. A cross section of the dewar is shown in Fig. 10 and an elevation view is shown in Fig. 11.

Refrigeration system

The superconducting accelerator will require a liquid helium refrigeration system with a cooling capacity of 14.2 kW at $1.85^{\circ} \pm 0.01$ °K. This capacity is based upon a design energy of 100 GeV and a duty cycle of $\frac{1}{16}$. It provides for the rf heat loss to the accelerator walls, anticipated beam losses, and refrigeration and dewar system losses. The presently planned refrigeration system is based upon a two-expansion-engine Claude cycle providing two stages of isobaric refrigeration at 60 to 70°K and 8 to 15°K temperature levels for a Linde-Hampton cycle which furnishes refrigeration at 1.85°K. Altogether, there will be 1 compressor

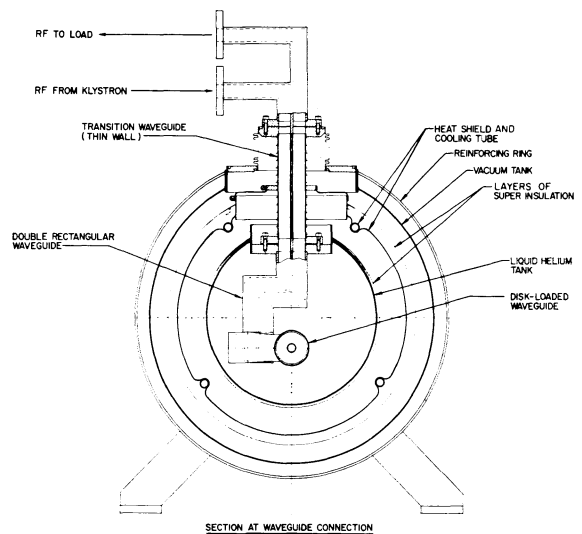


FIG. 10. Cross section of accelerator assembly.

station, 16 He I refrigerators, 32 He II refrigerators, and 16 vacuum pumping stations. Each He I refrigerator supplies two He II refrigerators with 10.2°K helium gas. At each sector the He II refrigerator will supply 1.85°K liquid helium to the dewars. The vaporized helium will be compressed to a pressure of 1.5 atmospheres by the vacuum pump and local compressor stations and returned to the main compressor station where the helium will be compressed to 12 atmospheres to complete the cycle.

Schedule of conversion program

A preliminary schedule for conversion of the two-mile accelerator to a superconducting version has been prepared. The program consists of three phases of work: research and development, preliminary design including the construction of a test accelerator, and final design and construction. Research and development began with a small materials study program in fiscal year 1968. This work was continued in fiscal years 1969 and 1970. The primary objective of this work is to provide a high degree of certainty regarding the technical feasibility of the superconducting accelerator. Once technical feasibility is established, the second phase of the program, preparation of preliminary designs and construction of a test accelerator, may start. The second phase can be accomplished in two years. Based upon the R and D program and early experience gained with the test accelerator, full authorization for the conversion program may

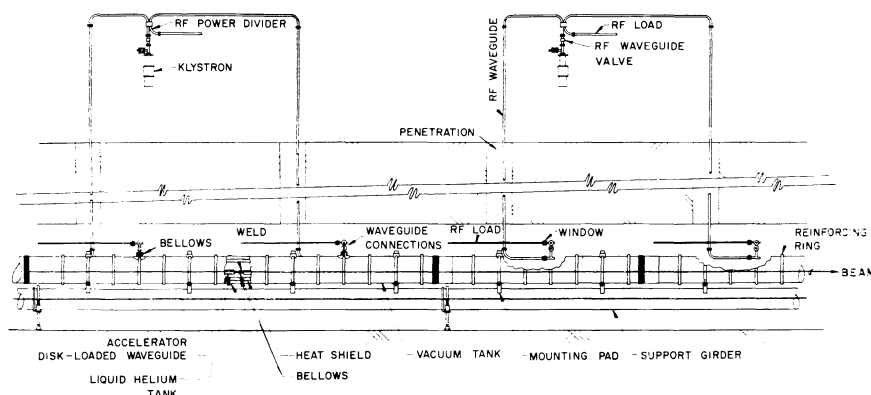


FIG. 11. Typical accelerator elevation.

be sought. As presently envisioned, five years will be required for completion of the final phase of the program. During the first three years following authorization, final designs will be procured, fabricated and stored temporarily. The existing accelerator will continue to be operated and a full experimental physics program will be conducted during this time. During the fourth year following authorization, operation of the existing machine will cease and installation of new hardware will take place. In the fifth year following authorization, checkout and testing of equipment will take place. Operations for experimental physics will commence the following year.

Cost estimates

Based upon conceptual and engineering data presently available, preliminary estimates of the cost of converting the two-mile SLAC accelerator to a superconducting machine have been prepared. The costs have been estimated in two categories: (1) research and development costs which will be obtained from the Laboratory's annual operating budgets, and (2) design and construction costs which require special Congressional authorization and appropriation actions. All estimates given in this report are based upon 1969 prices and do not include any allowances for price escalation in future years. The direct costs related to the R and D program will total approximately \$5 million. The total design and construction cost ranges between a minimum of \$66.9 and a maximum of \$78.5 million as shown in Table VI. The exact cost within these limits will depend upon the final feasibility of various design alternates which require further study. The above total cost estimates include 25 per cent contingency and are based upon

an operating frequency of 2856 MHz. As stated previously, the choice of 1428 MHz for the operating frequency would cost about 10 per cent more.

TABLE VI
Preliminary construction cost estimate for superconducting accelerator conversion (\$ millions)

	2856 MHz	
	Minimum	Maximum
I. Preliminary Design	4.000	4.000
II. Final Design and Construction		
1. Accelerator and mechanical structures	9.559	12.135
2. Beam dynamics	1.564	1.564
3. Injection	0.908	0.908
4. Positron source	1.840	1.840
5. Klystrons	2.626	2.626
6. Power supplies	0.707	0.707
7. Waveguide	4.549	4.549
8. Phase	2.212	2.212
9. Drive	1.204	1.304
10. Vacuum	1.388	1.892
11. Refrigeration	12.568	16.668
12. Electrical utilities	1.094	1.967
13. Cooling water	0.133	0.442
14. Beam switchyard	1.554	1.554
15. Instrumentation and control	2.932	2.932
16. Buildings	1.222	1.507
17. Project indirect costs	3.430	4.000
Sub Total	53.490	62.807
18. Contingency	13.370	15.703
Grand Total	66.860	78.510

Note: All estimates based upon calendar year 1969 prices. No allowances for price escalation are provided.

ACKNOWLEDGEMENTS

The contents of this progress report on superconducting accelerators at SLAC represent the work of many people distributed throughout the laboratory. Some of them have made and will continue to make contributions in specific areas of endeavor; others are acting in an overall advisory or administrative capacity. The authors would like to acknowledge the work of the following individuals: R. Miller for his contribution to accelerator structure design; J. V. Lebacqz and R. Stringall for their work on the cw klystron, G. Ratliff, F. Hall and S. St. Lorant for their contributions to the refrigeration system, V. Price, A. Keicher, R. Fowkes, Z. Farkas, T. C. McKinney, and H. Deruyter for their work on diverse microwave problems, A. Wilmunder on electronics, A. Lisin, R. Cochran, K. Welch and R. Sandkuhle on mechanical engineering, E. Hoyt and M. Rabinowitz on materials research, and L. Kral and C. Kruse for schedule and budget problems. In addition, the authors wish to thank the staff of the High Energy Physics Laboratory at Stanford University for frequent and useful discussions.

REFERENCES

1. *Feasibility Study for a Two-Mile Superconducting Accelerator*, Stanford Linear Accelerator Center, Stanford, California (revised December 1969), limited distribution.
2. J. P. Turneaure and N. T. Viet, Report No. HEPL-612, High Energy Physics Laboratory, Stanford University (October 1969). (Also to be published in *Appl. Phys. Letters*.)
3. For a summary, see for example, H. Alan Schwettman, 'The development of low temperature technology at Stanford and its relevance to high energy physics,' Proceedings of the 1968 Summer Study on Superconducting Devices and Accelerators, Brookhaven National Laboratory, p. 1, BNL 50155 (C-55),
4. J. P. Turneaure, Report No. HEPL-507, High Energy Physics Laboratory, Stanford University (May 1967).
5. M. Rabinowitz, 'Critical power dissipation in a superconductor', Report No. SLAC-PUB-708, Stanford Linear Accelerator Center, Stanford, California (January 1970). (To be published in *Appl. Phys. Letters*.)
6. J. Halbritter, 'The dependence of the surface impedance on the rf-field amplitudes', External Report No. 3/68-8, Kernforschungszentrum, Karlsruhe (October 1968).
7. H. Brechna and M. Rabinowitz, 'Thermal and electrical conductivity of niobium in the superconducting and normal states', Technical Note No. SLAC-TN-70-2, Stanford Linear Accelerator Center, in preparation.
8. W. F. Rich and M. D. J. MacRoberts, Report No. LA-4219, Los Alamos Scientific Laboratory, Los Alamos, New Mexico (September 1969).
9. H. C. Hoyt, *Rev. Sci. Instr.*, **37**, 755 (1966).
10. R. H. Helm (private communication).
11. T. M. Trainer, L. E. Hulbert, J. F. Lestingi, R. E. Keith *et al.*, 'NONLIN, A program from Batelle Memorial Institute', Technical Report No. AFRPL-TR-68-22, Air Force Rocket Propulsion Laboratory, Edwards, California (March 1968).
12. R. B. Neal, 'Consideration of the use of feedback in a traveling-wave superconducting accelerator' Proceedings of the 1968 Summer Study on Superconducting Devices and Accelerators, Part 1, Brookhaven National Laboratory, p. 111, BNL 50155 (C-55).
13. *Linear Accelerators*, edited by Pierre M. Lapostolle and Albert L. Septier (North Holland Publishing Company, Amsterdam, 1970), Chapter B.1.1, p. 97.
14. W. B. Herrmannsfeldt, H. A. Hogg, G. A. Loew and R. B. Neal, 'Feasibility study of a two mile superconducting linac', *IEEE Trans. Nucl. Sci.* **NS-16**, No. 3, 1004 (1969).
15. W. B. Herrmannsfeldt, G. A. Loew and R. B. Neal, 'Two-mile superconducting accelerator study', presented at the 7th International Conference on High Energy Accelerators, Yerevan, Armenia, USSR, Aug. 27-Sept. 2, 1969; Report No. SLAC-PUB-626, Stanford Linear Accelerator Center, Stanford, California (July 1969).

Received 27 April 1970